Heliyon 10 (2024) e31561

Contents lists available at ScienceDirect

Heliyon

journal homepage: www.cell.com/heliyon

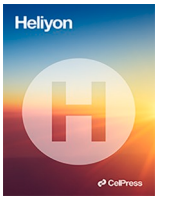

Research article

The joint action of yeast eisosomes and membraneless organelles in response to ethanol stress

Camila Moreira Pinto [a], Amanda Piveta Schnepper [a], Pedro Henrique Esteves Trindade [b], Luiz Henrique Cardoso [a], Matheus Naia Fioretto [c], Luís Antônio Justulin [c], Cleslei Fernando Zanelli [d], Guilherme Targino Valente [a,*]

[a] Laboratory of Applied Biotechnology. São Paulo State University (UNESP). Botucatu, Brazil
[b] Department of Population Health and Pathobiology College of Veterinary Medicine, North Carolina State University (NCSU) Raleigh, USA
[c] Department of Structural and Functional Biology, Institute of Biosciences. São Paulo State University (UNESP). Botucatu, Brazil
[d] Department of Biological Science, São Paulo State University (UNESP), Araraquara, Brazil

ARTICLE INFO

Keywords:
Eisosomes
Proton flux
Cell stressor
Membrane compartments
P-bodies
Stress granules
Saccharomyces cerevisiae
Ethanol tolerance

ABSTRACT

Elevated ethanol concentrations in yeast affect the plasma membrane. The plasma membrane in yeast has many lipid-protein complexes, such as Pma1 (MCP), Can1 (MCC), and the eisosome complex. We investigated the response of eisosomes, MCPs, and membraneless structures to ethanol stress. We found a correlation between ethanol stress and proton flux with quick acidification of the medium. Moreover, ethanol stress influences the symporter expression in stressed cells. We also suggest that acute stress from ethanol leads to increases in eisosome size and SG number: we hypothesized that eisosomes may protect APC symporters and accumulate an mRNA decay protein in ethanol-stressed cells. Our findings suggest that the joint action of these factors may provide a protective effect on cells under ethanol stress.

1. Introduction

Ethanol is one of the most critical stressors for *Saccharomyces cerevisiae* during fermentation [1]. Ethanol alters the fluidity and permeability of the plasma membrane, altering the pH of the cytosol and the intake of nutrients. Consequently, ethanol stress quickly dampens cell division and cell surveillance [1–6].

The plasma membrane of *S. cerevisiae* has several lipid-protein complexes, including the PMA1 (MCP) and Can1 (MCC) membrane compartments [7,8]. The H^+-ATPase PMA1 protein is a component of MCP, which regulates proton efflux to maintain intracellular pH and nutrient uptake [9]. The eisosome protein complex is associated with MCC [10]. Pil1p is essential for the yeast MCC/eisosome complex [11]. Eisosomes resemble "stationary" punctate patches associated with membrane invaginations, forming grooves approximately 50 nm deep to 300 nm long [12]. This region is enriched in phosphatidylinositol 4,5-bisphosphate [PI(4,5)P2] lipids bound to eisosome proteins (such as Pil1, Lsp1, and Slm1/2) [13–15]. MCC/eisosomes can accumulate ergosterol [8], and amino acid-polyamine-organocation (APC) symporters responsible for the influx of ions and nutrients [7–9,11,12,16–21]. In response to a variety of stressors, eisosomes engage in multiple cell signaling pathways and interact with numerous structures [10,20].

* Corresponding author.
E-mail address: valentegt@gmail.com (G.T. Valente).

https://doi.org/10.1016/j.heliyon.2024.e31561
Received 4 March 2024; Received in revised form 13 May 2024; Accepted 17 May 2024
Available online 19 May 2024

P-bodies (PBs) and stress granules (SGs) are membraneless structures assembled in cells under glucose starvation, accumulation of reactive oxygen species, cell acidification, and other conditions. These structures help cells cope with stressors until stress relief [22–24].

Some membrane proteins are responsive to stresses in yeasts. For instance, the abundance of Pil1p increases in yeast *Yarrowia lipolytica* subjected to osmotic stress [25], V-ATPase is associated with ethanol stress in *S. cerevisiae* [26], and membrane-related genes were differentially expressed in *S. cerevisiae* under ethanol stress [22]. Furthermore, proteins related to PBs and SGs responded to ethanol stress in *S. cerevisiae* BMA64-1A and S288C strains [22].

Although many studies have focused on the plasma membrane compartments of *S. cerevisiae*, little is known about the joint action of eisosomes, MCP, and membraneless structures in cells under acute ethanol stress. Here, we investigated the relationship between eisosomes, ethanol stress, proton efflux, PB, and SG. By analyzing cells exposed to different concentrations of ethanol, we found that ethanol stress influences symporter expression. Furthermore, we suggest that acute stress from ethanol leads to increases in eisosome size and SG number. In this case, we hypothesize that eisosomes may protect APC symporters and accumulate an mRNA decay protein in ethanol-stressed cells. Altogether, we suggest that the coordinated action of the eisosome and SGs during ethanol stress may be a stress response mechanism that helps yeast endure ethanol stress.

2. Material and methods

2.1. Selected strains and workflow

S. cerevisiae BY4741 wild-type (MATa his3Δ1 leu2Δ0 met15Δ0 ura3Δ0) (hereafter referred to as BY4741-WT) was obtained from Euroscarf, and BY4741 with open reading frames (ORFs) coupled with green fluorescent proteins (GFP) (hereafter referred to as

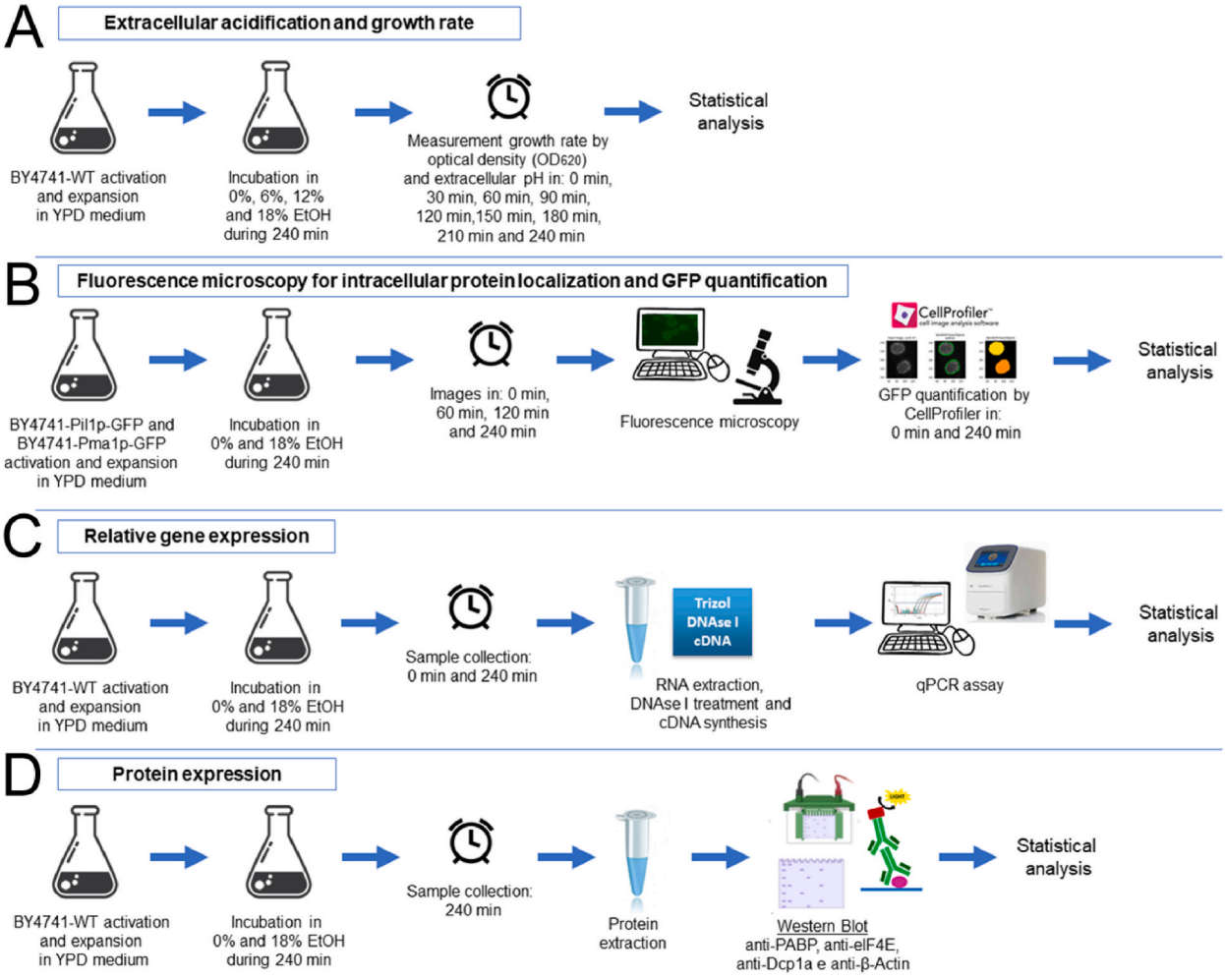

Fig. 1. An overview of this study. **A:** experiments of extracellular acidification and growth rate; **B:** experiments of fluorescent microscopy; **C:** gene expression analysis; **D:** analysis of protein expression. **EtOH:** ethanol.

BY4741-GFP) was obtained from Invitrogen [27]. Medium acidification, cell microscopy, RNA, and protein expression analyses were performed in both types of strains mentioned (Fig. 1).

2.2. Medium acidification analysis and subcellular localization of Pil1 and Pma1 proteins

The strains were grown in YPD medium (2 % peptone, 1 % yeast extract and 2 % glucose) at 30 °C and 200 RPM for ~16 h. OD_{620} was estimated with the Asys Expert Plus Microplate Reader (Biochrom), and the cell concentration was adjusted to an OD_{620} of 0.4 before all experiments.

The acidification of the medium was also estimated. In this case, the BY4741-WT strain was grown in YPD (30 °C and 200 RPM) with 0 %, 6 %, 12 % and 18 % ethanol (v/v). The samples were collected at 0, 30, 60, 90, 120, 150, 180, 210, and 240 min of incubation: the 'time 0 min samples' were collected soon after incubation. The OD_{620} of each sample was quantified and the external pH was measured using a PG2000 (Gehaka).

The subcellular location of the Pil1 and Pma1 proteins was independently evaluated in biological duplicates (samples independently cultivated). The BY4741-Pil1p-GFP and BY4741-Pma1p-GFP strains were grown in YPD (30 °C and 200 RPM) with 0 % and 18 % ethanol (v/v). The samples were collected at 0, 60, 120, and 240 min of incubation. Two hundred microliters of each sample were centrifuged (2000 RPM for 2 min), washed twice with 100 μL of PBS and centrifuged (2000 RPM for 2 min). The pellet was resuspended in 50 μL of PBS and 20 μL of cells was dropped onto optical microscopy slides. Cell images were captured using an Olympus BX61 optical fluorescence microscope with a FITC filter and a 5 μm scale. The subcellular location and quantification of GFP of the Pil1 and Pma1 proteins of 10 cells per biological replicate (samples independently cultivated), totalizing 20 cells per time point and condition, were performed using CellProfiler V. 4.2.1 [28] (Supplementary Fig. S1). The images were treated neither during nor after capture.

2.3. RT–qPCR analysis and Western blot

The expression of selected genes and proteins was quantified in BY4741-WT grown in YPD with 0 % and 18 % ethanol (v/v). Samples were collected at 0 and 240 min of incubation to quantify the expression of selected genes by qPCR (Table 1) and at 240 min to quantify proteins related to mRNA degradation machinery and PB and SG by Western blot.

For RNA extraction, collected samples (biological triplicates, which were samples independently cultivated) were centrifuged (2000 RPM for 2 min), the supernatant was discarded, and the pellet was immediately frozen at −80 °C to cease growth. Cells were treated at 30 °C for 30 min with 250 μL of Lyticase prepared with 1 M sorbitol, 0.1 M EDTA, and 0.1 μL of β-mercaptoethanol. Then, total RNA was extracted using TRIzol (Invitrogen). The RNA concentration was estimated using the Qubit RNA BR Assay Kit and the Qubit 3.0 Fluorometer (Thermo Fisher Scientific). RNA (1 μg) was treated with DNase I – Amplification Grade (Invitrogen). cDNA was synthesized using a High Capacity cDNA kit (Applied Biosystems). We followed the manufacturer's instructions for all kits used here.

The expression of selected genes (Table 1) was quantified using SYBR Green and a QuantStudio 3 real-time PCR system thermocycler (Thermo Fisher Scientific). The reaction setup was 7.5 μL of GoTaq qPCR Master Mix (Promega), 1 μL of forward oligo (5 μM), 1 μL of reverse oligo (5 μM), 2 μL of cDNA (1:5 diluted) and 3.5 μL of water. The PCR cycle was 95 °C for 2 min, followed by 40 cycles of 95 °C for 3 s and 60 °C for 30 s. The melting curve of each gene was evaluated according to the GoTaq qPCR Mastermix protocol (Promega). The expression of the endogenous *TDH2* gene [29] (Table 1) was quantified in all assays and used to normalize the expression of selected genes. The relative expression of each gene was calculated using the ΔΔCt method [30] and corrected for by the amplification reaction efficiency using the equation described by Pfaffl [31].

We examined the levels of DCP1a (a PB marker), PABP (an SG marker), and eIF4E (a translation stalling marker) proteins by Western blotting. For protein extraction, 20 ml of sample (six biological replicates, which were samples independently cultivated) was centrifuged at 2000 RPM for 3 min. The supernatant was discarded and the pellet was resuspended with 600 μL of lithium acetate (2.0 M) with 200 μL of NaOH (0.4 M). The samples were allowed to stand for 5 min on ice and centrifuged at 2000 RPM for 1 min. The supernatant was discarded and the protein abundance was quantified using the Bradford method [32]. Seventy micrograms of protein were subjected to electrophoresis in a 10 % polyacrylamide gel, transblotted onto a Hybond ECL nitrocellulose membrane (Amersham, Little Chalfont), and blocked in 5 % fat-free milk for 1 h. The membranes were then incubated with the specific primary antibodies anti-DCP1a (sc-100706; Santa Cruz, 1:1000), anti-PABP (sc-166027, Santa Cruz, 1:1000), and anti-eIF4E (sc-9976, Santa Cruz,

Table 1
Oligonucleotides used in the qPCR analysis. Fw: forward; **Rw:** reverse.

Gene (amplicon length)	SGD ID		Sequence (5′-3′)	Usage
TDH2 (90 bp)	**YJR009C**	Fw	AGACTGTTGACGGTCCATCC	Endogenous
		Rw	CCTTAGCAGCACCGGTAGAG	
PIL1 (118 bp)	**YGR086C**	Fw	AGAAGTGCTGCTGGAGCTTT	MCC/eisosomes
		Rw	CAGCGTCACGTCTTTCGTTG	
CAN1 (99 bp)	**YEL063C**	Fw	AGACGCCGACATAGAGGAGA	Proton gradient
		Rw	ATTGACCCACGTCTGTGGTG	
PMA1 (108 bp)	**YGL008C**	Fw	GGTCAAAGCGTCCTTAGCCT	MCP, proton gradient
		Rw	TTGACTGCTTGTTTGGCTGC	
XRN1 (127 bp)	**YGL173C**	Fw	TGGTTGGGGGTCCTATTCCT	mRNA decay
		Rw	GGGTAAGGCATCTGGTGAGG	

1:1000): anti-DCP1 was used to assess the abundance of DCP1 (responsible for mRNA degradation machinery and PB), anti-PABP to infer the abundance of SG (responsible for holding mRNAs), and anti-eIF4E to infer translation stalling by SG. The membrane was washed with TBS and incubated with rabbit anti-mouse secondary antibody (Abcam-ab6709) (1:5000 for 2 h), followed by a final wash with TBS. Reactions were performed using an ECL kit (Amersham, USA), molecular weight was determined by comparison with a standard kaleidoscope (Bio-Rad), and signals were captured using a CCD camera (ImageQuant 350 GE Healthcare). The integrated optical densities of the targeted protein bands were measured using ImageJ software (National Institutes of Health). The expression level of each protein was normalized according to β-actin (Abcam-8226) (1:1000), and the results are expressed as the fold change as the mean ± SD.

2.4. Statistical analyses

Statistical analyses were performed using the RStudio environment V. 4.1.0 [33] considering 5 % significance. Residual errors in all models showed a Gaussian distribution according to the Cramer-Von Mises test, with BY4741-Pil1p-GFP and BY4741-Pma1p-GFP quantification being the only exception: these data were submitted to the Box–Cox method transformation ($\lambda = -7.975458$ and $\lambda = -5.239547$ respectively) for the Gaussian distribution fit. Multiple comparisons were performed for all models using the post hoc test with Tukey's test. We considered the percentages of ethanol and the time points as fixed effects for the simple linear and mixed linear models used here and the biological replicates (samples independently cultivated) as random effects in mixed linear models.

The pH values of samples under different conditions (0 %, 6 %, 12 % and 18 % ethanol (v/v)) were compared to each other using mixed linear models; the same procedure was applied to compare OD_{620}. The same models were also applied to compare different time points versus the initial time (0 h). The Pearson coefficient correlation between pH and OD_{620} was also estimated.

The average Pil1p and Pma1p GFP intensities were calculated independently for each time point (0 min and 240 min) and condition (0 % and 18 % ethanol (v/v)). A mixed linear model compared the averages between the conditions and between the time points.

A simple linear model estimated the significance of $2^{\Delta\Delta Ct}$ standardized values for the PIL1, CAN1, PMA1 and XRN1 genes by comparing the time points (0 vs. 240 min). The $2^{\Delta\Delta Ct}$ normalization to allow inter-sample comparison was conducted first for the control group based on the Z score method, followed by the treatment group based on the control normalized values.

The average of the Western blot data for each protein (DCP1a, PABP, and eIF4E) normalized to β-actin was calculated for both conditions (0 % and 18 % ethanol (v/v)). The two-tailed paired *t*-test was used to estimate the significance of the differences for each protein.

3. Results

3.1. Rationale

By analyzing the location of fluorescent proteins in cells, cell growth profiles, extracellular acidification, and mRNA and protein yields, we investigated the response of eisosomes, MCPs, and membraneless structures in cells under ethanol stress (Fig. 1).

Medium acidification is common for a yeast that grows in a glucose-rich medium [34]. Similarly, we previously observed that yeast strains BMA64-1A and S288C under ethanol stress acidified the medium. Based on our transcriptome analysis, we also observed an enrichment of terms related to eisosomes [22]. Eisosomes indirectly affect membrane potential by aggregating APCs [8,9,21]. We first hypothesized that with elevated ethanol stress, eisosomes participate in the membrane potential or cellular homeostasis. The efflux of protons was evidenced here in the BY4741 strain by testing the acidification of the growth medium and the growth rate at various levels of ethanol stress.

Pil1p and Can1p are components of the MCC/eisosome complex [11]. Pma1p is the main proton efflux-related protein [35]. We used microscopy and quantitative PCR (qPCR) to determine the intracellular location and abundance of PIL1 and PMA1; CAN1 was only examined using qPCR to avoid misinterpretation related to the PIL1 signal in microscopy analysis. We hypothesized that the levels of PMA1, PIL1, and CAN1 and their subcellular location would be altered in BY4741 under ethanol stress since ethanol affects membrane fluidity [36].

Xrn1p is responsible for mRNA degradation, is a component of P-bodies (PBs), and may anchor at or in the close vicinity of eisosomes in postdiauxic shift cells [37]. PB, stress granules (SGs) and translation stalling are responsible for the post-transcriptional regulation of mRNA levels in stressed yeast cells [24]. Therefore, we were also interested in determining whether ethanol stress influences protein levels through eisosomes. We used qPCR to determine the level of XRN1 and Western blotting to determine protein levels of Dcp1ap (a PB marker), PABP (an SG marker), and Elf4E (a translation stalling marker).

3.2. Growth and proton efflux analyses

The growth of the yeast population is slower as the levels of ethanol stress increase. For example, cells treated with 6 % ethanol increased their growth rate at 90 min, cells treated with 12 % ethanol increased their growth at ~120 min, and cells treated with 18 % ethanol maintained their growth in the lag phase (Fig. 2A). Similarly, extracellular acidification was less extensive as ethanol levels increased: medium with cells and 6 % ethanol significantly accelerated acidification after 30 min, at 12 % ethanol reduced external pH after ~60 min, and after 150 min with 18 % ethanol (Fig. 2B). Therefore, we found a significant negative correlation between OD_{620} and extracellular pH (Fig. 2C–E).

3.3. Quantification of genes and proteins

We investigated the subcellular location of PIL1 and PMA1 in control and in cells treated with ethanol. We observed a distribution profile of Pma1p throughout the cell internalized over time in untreated cells (Fig. 3A). The Pil1p distribution profile is similar in cells regardless of the presence of ethanol or the time of stress exposure; this protein is distributed on the periphery of the plasma membrane (Fig. 3B).

We investigated the relationship between the fluorescence intensity of Pma1p and Pil1p and their intracellular localization. The intensities of Pil1p GFP presented a slight reduction after 240 min of incubation without ethanol and an increase after 240 min of incubation with ethanol. There was no significant difference when comparing the starting point (0 min) with and without ethanol. The intensities of the Pma1p GFP did not exhibit a significant modification (Fig. 4A–B).

The expression of the CAN1, XRN1, and PIL1 genes increased significantly in cells after 240 min of incubation with 18 % ethanol, while PMA1 decreased gene expression under the same conditions (Fig. 4C–F). PMA1 gene expression was reduced in cells treated with 18 % ethanol after 240 min (Fig. 4F).

PB, SG, and translation stalling are responsible for mRNA/protein metabolism [24]. The purpose of analyzing these structures and processes was to better evaluate the apparent relationship between proton efflux, eisosomes, and mRNA levels: based on XRN1 expression data measured here, we suggest a relationship between proton efflux, mRNA metabolism, and eisosomes (Fig. 4E). The abundance of Dcp1a protein (PB marker) decreased in cells under 18 % ethanol stress, while the abundance of PABP (SG marker) and eIF4E (translation stalling marker) increased under the same conditions (Fig. 4G–I; Supplementary Fig. S2).

4. Discussion

An overview of our conclusions discussed below is presented in Fig. 5.

Yeast grown in a glucose-rich medium rapidly acidifies the extracellular environment [34]. Similar to previous studies, the higher concentration of ethanol tested here induced a stationary growth phase [1,22,38–40] and reduced proton efflux, indicating acidification of the cytosol [22]. In fact, our external pH levels are similar to those previously found [26].

The efflux of protons from cells is dependent on the activity of Pma1p (MCP) [9,41]. The level of PMA1 expression was downregulated in cells under heat stress, affecting its activity [33]. Here, we observed that chronic exposure to high levels of ethanol decreased the expression of the PMA1 gene. However, Pma1p is a long-lived protein [42], and therefore we are expected to find no significant modification in Pma1p-GFP measurement, such as observed here. Furthermore, mutations or specific ubiquitination alter Pma1p recruitment to rafts, which diverts Pma1p from the plasma membrane to the vacuoles [43,44]. Our current data did not allow us to determine whether PMA1 was indeed present in vacuoles. Further analysis using Western blot or immunofluorescence could help to better understand the relationship between Pma1p, vacuoles, and ethanol stress.

A higher level of PIL1 resulted in a normal density of larger-sized eisosomes [45]. Furthermore, cells in the stationary phase had an

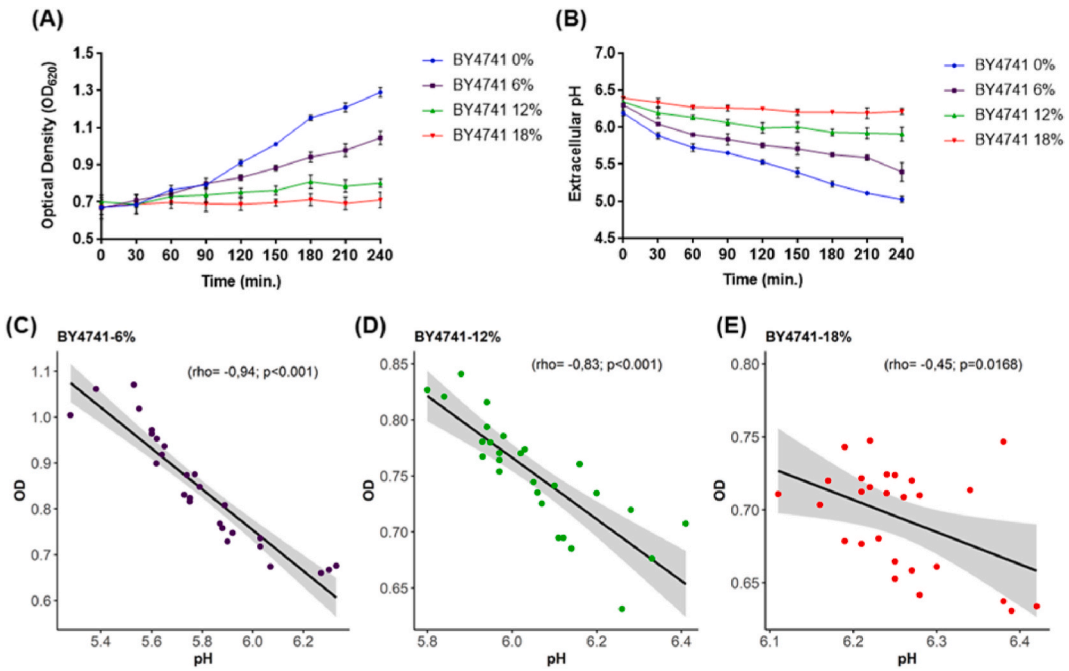

Fig. 2. Analysis of population growth and extracellular acidification. **A:** population growth analysis; **B:** extracellular pH; **C-E:** Pearson coefficient correlation with the confidence interval (gray areas).

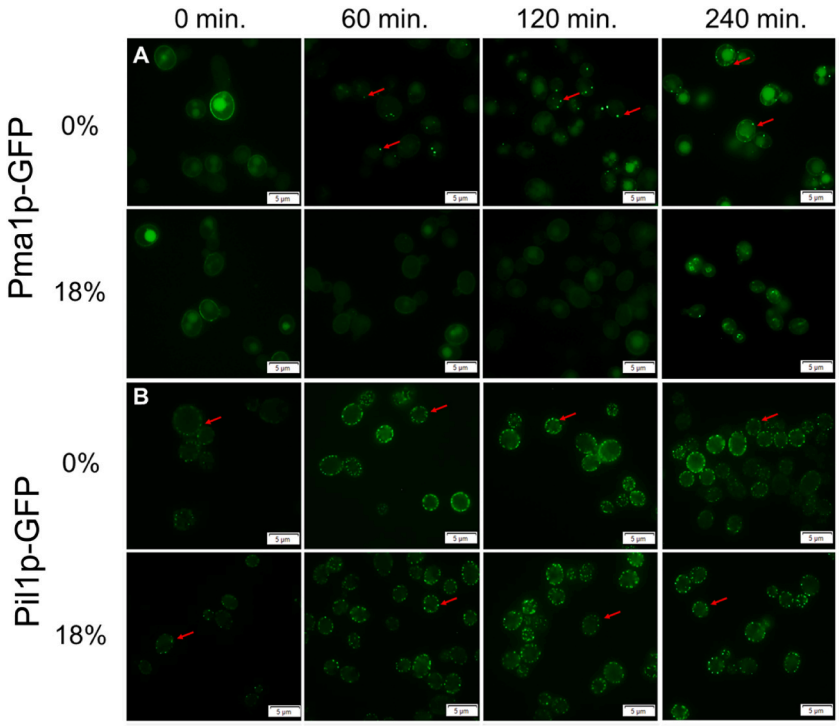

Fig. 3. Analysis of the subcellular location of Pma1p and Pil1p in BY4741-GFP strains. **A:** BY4741-Pma1p-GFP strain. Pma1p is evidenced as lighter green dots dispersed in the cytosol and plasma membrane; **B:** BY4741-Pil1p-GFP strain. Pil1p is shown as green dots on the plasma membrane. The arrows indicate some Pma1p or Pil1p. The percentages on the left side indicate the ethanol concentration (v/v) analyzed.

increase in the number and size of MCC/eisosomes [9,46]. Here, we observed an increase in PIL1 (Pil1p is part of the MCC/eisosome) expression and protein abundance in ethanol-stressed cells at stationary phase growth. Therefore, our data indirectly suggest that the ethanol stress analyzed here induces the normal formation of large-sized eisosomes.

PBs and SGs jointly regulate mRNA translation and decay [37,47]. PB captures untranslated mRNA, Dcp1ap, Xrn1p, and other molecules [48]. SG captures translation-related molecules, including Pab1 [48,49]. The XRN1 gene is a component of eisosomes in postdiauxic cells [37]. The inactive form of XRN1 stored in eisosomes prevents unnecessary degradation of potentially relevant mRNAs for post-stressed cells [50]. Therefore, we investigated the relationship between ethanol stress, membraneless organelles, and eisosomes, hypothesizing that eisosomes protect cells exposed to chronic ethanol stress.

We previously found that ethanol-stressed BY4741 activates the diauxic shift mechanisms by reducing glucose intake [22]. Glucose depletion (glucose starvation) induces the assembly of membraneless organelles (e.g., PB and SG) [22–24]. The diauxic shift induces the relocation of Xrn1p from PBs to eisosomes, reducing mRNA decay by inactivating this protein [37,50]. The relocation of Xrn1p to eisosomes is a Pil1p-dependent mechanism [50]. We observed a reduction in the yield of Dcp1p and an induction of PABP, XRN1 and Pil1p in cells with chronic exposure to ethanol. These results allowed us to hypothesize that chronic ethanol stress reduces the number of PBs, increases the number of SGs and likely leads to accumulation of Xrn1p in eisosomes in a Pil1p-dependent manner.

SGs allow for faster cell growth after stress relief [24,47,51]. Therefore, we suggest that the previously proposed model [47] applies to cells under ethanol stress: eisosomes stimulate the assembly of SG, allowing a faster population rebound after stress by holding inactive XRN1 for further release.

The combination of different approaches focusing on studying the role of eisosomes in ethanol-stressed cells allowed us to assess the spatial and functional dynamism of these structures. Therefore, we hypothesize that eisosomes play a role in the surveillance of yeast cells under ethanol stress by acting on intracellular homeostasis, protecting symporters, and working on mRNA metabolism.

Funding

This work was supported by São Paulo Research Foundation (FAPESP) [grant numbers 2015/12093-9 and 2017/08463-0].

Data availability statement

All data to support the conclusions have been presented as Supplementary Materials and in the Figshare database (https://figshare.com/s/731bc29e0a732d51dc86 and https://figshare.com/s/290200c766d2ea5df8ae).

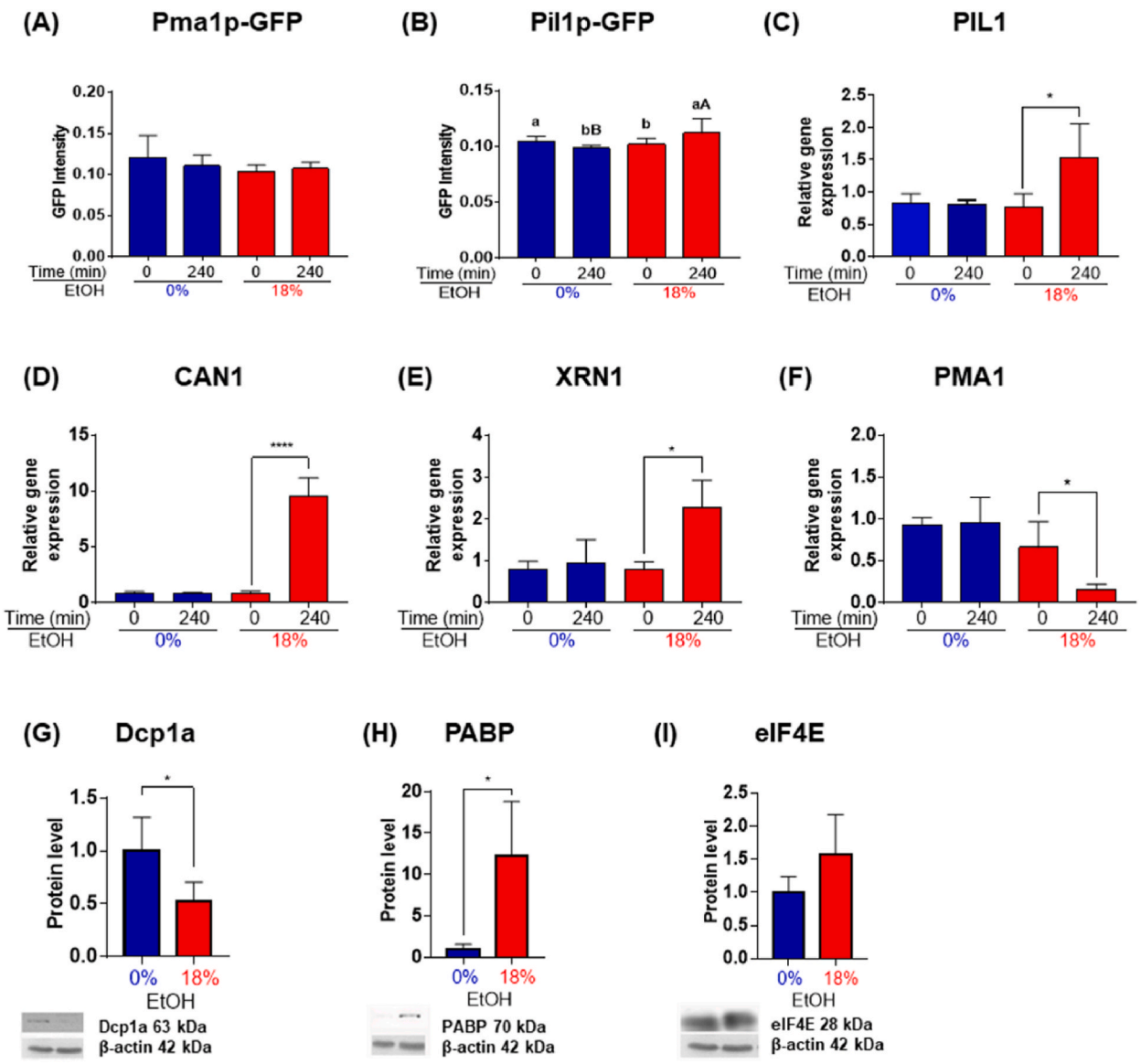

Fig. 4. Bar plots of gene expression, GFP fluorescence, and protein abundance. **A-B:** Quantification of the GFP intensity of thePma1 and Pil1 proteins (the raw data are available in Table S1). Multiple comparisons in the post hoc test were conducted for the intensities of Pma1p and Pil1p GFP. Different lowercase letters (a>b) indicate significant differences between the time points for the same treatment. Different capital letters (A > B) indicate significant differences between treatments within the time point based on Tukey's test. Different bars with equal lowercase or capital letters indicate non-significant differences. The divergent letters above each bar in the Tukey's test indicate statistically significant average differences; **C–F:** quantification of the PIL1, CAN1, XRN1 and PMA1 mRNAs by qPCR; **G-I:** quantification of the Dcp1a, PABP and eIF4E proteins by Western blot analysis of samples incubated for 240 min. Samples were blotted simultaneously in a single membrane; **EtOH:** ethanol. The "*" p value < 0.05 and "***" p value < 0.001. We used 10 cells per biological replicate (samples independently cultivated), three samples, and six samples as biological replicates (samples independently cultivated) for GFP (Supplementary Table S1, https://figshare.com/s/731bc29e0a732d51dc86 and https://figshare.com/s/290200c766d2ea5df8ae), qPCR and Western blot analysis (the uncropped blots can be found in Supplementary Fig. S2), respectively. Multiple comparisons were made for all models using the post hoc test with the Tukey's test. The two-tailed paired *t*-test was used to estimate the significance of the differences for each protein in Western blot.

CRediT authorship contribution statement

Camila Moreira Pinto: Writing – review & editing, Writing – original draft, Validation, Methodology, Investigation, Formal analysis, Conceptualization. **Amanda Piveta Schnepper:** Formal analysis. **Pedro Henrique Esteves Trindade:** Formal analysis. **Luiz Henrique Cardoso:** Formal analysis. **Matheus Naia Fioretto:** Writing – original draft, Formal analysis. **Luís Antônio Justulin:** Formal analysis. **Cleslei Fernando Zanelli:** Resources, Formal analysis. **Guilherme Targino Valente:** Writing – review & editing,

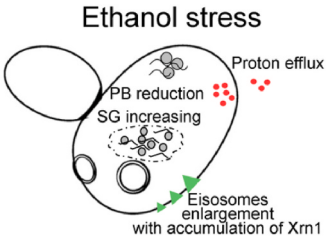

Fig. 5. An overview of our conclusions.

Writing – original draft, Supervision, Project administration, Funding acquisition, Formal analysis, Conceptualization.

Declaration of competing interest

The authors declare that they have no known competing financial interests or personal relationships that could have appeared to influence the work reported in this paper.

Acknowledgments

The authors thank Dr. Adauto Cardoso of Sao Paulo State University (Brazil) for supervising the optical microscopy images.

Appendix A. Supplementary data

Supplementary data to this article can be found online at https://doi.org/10.1016/j.heliyon.2024.e31561.

References

[1] D. Stanley, A. Bandara, S. Fraser, P.J. Chambers, G.A. Stanley, The ethanol stress response and ethanol tolerance of Saccharomyces cerevisiae, J. Appl. Microbiol. 109 (2010) 13–24, https://doi.org/10.1111/j.1365-2672.2009.04657.x.
[2] M. Chandler, G. a Stanley, P. Rogers, P. Chambers, A genomic approach to defining the ethanol stress response in the yeast Saccharomyces cerevisiae, Ann. Microbiol. 54 (2004) 427–454.
[3] J. Ding, X. Huang, L. Zhang, N. Zhao, D. Yang, K. Zhang, Tolerance and stress response to ethanol in the yeast Saccharomyces cerevisiae, Appl. Microbiol. Biotechnol. 85 (2009) 253–263, https://doi.org/10.1007/s00253-009-2223-1.
[4] M. Ma, Z.L. Liu, Mechanisms of ethanol tolerance in saccharomyces cerevisiae, Appl. Microbiol. Biotechnol. 87 (2010) 829–845, https://doi.org/10.1007/s00253-010-2594-3.
[5] K. Jia, Y. Zhang, Y. Li, Systematic engineering of microorganisms to improve alcohol tolerance, Eng. Life Sci. 10 (2010) 422–429, https://doi.org/10.1002/elsc.201000076.
[6] E. Navarro-Tapia, R.K. Nana, A. Querol, R. Pérez-Torrado, Ethanol cellular Defense induce unfolded protein response in yeast, Front. Microbiol. 7 (2016), https://doi.org/10.3389/fmicb.2016.00189.
[7] L.M. Douglas, H.X. Wang, L. Li, J.B. Konopka, Membrane compartment Occupied by Can1 (MCC) and eisosome Subdomains of the Fungal plasma membrane, Membranes 1 (2011) 394–411, https://doi.org/10.3390/membranes1040394.
[8] G. Grossmann, M. Opekarová, J. Malinsky, I. Weig-Meckl, W. Tanner, Membrane potential governs lateral segregation of plasma membrane proteins and lipids in yeast, EMBO J. 26 (2007) 1–8, https://doi.org/10.1038/sj.emboj.7601466.
[9] J.V. Busto, R. Wedlich-Söldner, Integration through separation – the role of lateral membrane segregation in nutrient uptake, Front. Cell Dev. Biol. 7 (2019), https://doi.org/10.3389/fcell.2019.00097.
[10] L.M. Douglas, J.B. Konopka, Fungal membrane organization: the eisosome concept, Annu. Rev. Microbiol. 68 (2014) 377–393, https://doi.org/10.1146/annurev-micro-091313-103507.
[11] T.C. Walther, J.H. Brickner, P.S. Aguilar, S. Bernales, C. Pantoja, P. Walter, Eisosomes mark static sites of endocytosis, Nature 439 (2006) 998–1003, https://doi.org/10.1038/nature04472.
[12] V. Strádalová, W. Stahlschmidt, G. Grossmann, M. Blažíková, R. Rachel, W. Tanner, J. Malinsky, Furrow-like invaginations of the yeast plasma membrane correspond to membrane compartment of Can1, J. Cell Sci. 122 (2009) 2887–2894, https://doi.org/10.1242/jcs.051227.
[13] N.E. Ziółkowska, L. Karotki, M. Rehman, J.T. Huiskonen, T.C. Walther, Eisosome-driven plasma membrane organization is mediated by BAR domains, Nat. Struct. Mol. Biol. 18 (2011) 854–856, https://doi.org/10.1038/nsmb.2080.
[14] L. Karotki, J.T. Huiskonen, C.J. Stefan, N.E. Ziółkowska, R. Roth, M.A. Surma, N.J. Krogan, S.D. Emr, J. Heuser, K. Grünewald, T.C. Walther, Eisosome proteins assemble into a membrane scaffold, J. Cell Biol. 195 (2011) 889–902, https://doi.org/10.1083/jcb.201104040.
[15] J.E. Foderaro, L.M. Douglas, J.B. Konopka, MCC/Eisosomes regulate cell wall synthesis and stress responses in fungi, J. Fungi 3 (2017) 61, https://doi.org/10.3390/jof3040061.
[16] F. Bianchi, J.S. van't Klooster, S.J. Ruiz, B. Poolman, Regulation of amino acid transport in Saccharomyces cerevisiae, Microbiol. Mol. Biol. Rev. 83 (2019), https://doi.org/10.1128/MMBR.00024-19.
[17] M.H. Saier, V.S. Reddy, B.V. Tsu, M.S. Ahmed, C. Li, G. Moreno-Hagelsieb, The transporter classification database (TCDB): recent advances, Nucleic Acids Res. 44 (2016) D372–D379, https://doi.org/10.1093/nar/gkv1103.
[18] K. Malínská, J. Malínský, M. Opekarová, W. Tanner, Visualization of protein compartmentation within the plasma membrane of living yeast cells, Mol. Biol. Cell 14 (2003) 4427–4436, https://doi.org/10.1091/mbc.e03-04-0221.
[19] K. Malinska, J. Malinsky, M. Opekarova, W. Tanner, Distribution of Can1p into stable domains reflects lateral protein segregation within the plasma membrane of living S. cerevisiae cells, J. Cell Sci. 117 (2004) 6031–6041, https://doi.org/10.1242/jcs.01493.

[20] C.E. Lanze, R.M. Gandra, J.E. Foderaro, K.A. Swenson, L.M. Douglas, J.B. Konopka, Plasma membrane MCC/eisosome domains promote stress resistance in fungi, Microbiol. Mol. Biol. Rev. 84 (2020), https://doi.org/10.1128/MMBR.00063-19.

[21] A. Moharir, L. Gay, D. Appadurai, J. Keener, M. Babst, Eisosomes are metabolically regulated storage compartments for APC-type nutrient transporters, Mol. Biol. Cell 29 (2018) 2113–2127, https://doi.org/10.1091/mbc.E17-11-0691.

[22] I.R. Wolf, L.F. Marques, L.F. de Almeida, L.C. Lázari, L.N. de Moraes, L.H. Cardoso, C.C. de O. Alves, R.T. Nakajima, A.P. Schnepper, M. de A. Golim, T. R. Cataldi, J.G. Nijland, C.M. Pinto, M.N. Fioretto, R.O. Almeida, A.J.M. Driessen, R. Plana Simões, M.V. Labate, R.M.T. Grotto, C.A. Labate, A. Fernandes Junior, L.A. Justulin, R.L.B. Coan, É. Ramos, F.B. Furtado, C. Martins, G.T. Valente, Integrative analysis of the ethanol tolerance of Saccharomyces cerevisiae, Int. J. Mol. Sci. 24 (2023) 5646, https://doi.org/10.3390/ijms24065646.

[23] J.R. Buchan, J.H. Yoon, R. Parker, Stress-specific composition, assembly and kinetics of stress granules in Saccharomyces cerevisiae, J. Cell Sci. 124 (2011) 228–239, https://doi.org/10.1242/jcs.078444.

[24] W. van Leeuwen, C. Rabouille, Cellular stress leads to the formation of membraneless stress assemblies in eukaryotic cells, Traffic (2019) 12669, https://doi.org/10.1111/tra.12669 tra.

[25] M. Kubiak-Szymendera, B. Skupien-Rabian, U. Jankowska, E. Celińska, Hyperosmolarity adversely impacts recombinant protein synthesis by Yarrowia lipolytica—molecular background revealed by quantitative proteomics, Appl. Microbiol. Biotechnol. 106 (2022) 349–367, https://doi.org/10.1007/s00253-021-11731-y.

[26] S. Charoenbhakdi, T. Dokpikul, T. Burphan, T. Techo, C. Auesukaree, Vacuolar H + -ATPase protects Saccharomyces cerevisiae cells against ethanol-induced oxidative and cell wall stresses, Appl. Environ. Microbiol. 82 (2016) 3121–3130, https://doi.org/10.1128/AEM.00376-16.

[27] W.-K. Huh, J.V. Falvo, L.C. Gerke, A.S. Carroll, R.W. Howson, J.S. Weissman, E.K. O'Shea, Global analysis of protein localization in budding yeast, Namsture 425 (2003) 686–691, https://doi.org/10.1038/nature02026.

[28] T.R. Jones, I.H. Kang, D.B. Wheeler, R.A. Lindquist, A. Papallo, D.M. Sabatini, P. Golland, A.E. Carpenter, CellProfiler Analyst: data exploration and analysis software for complex image-based screens, BMC Bioinf. 9 (2008) 482, https://doi.org/10.1186/1471-2105-9-482.

[29] E. Vaudano, O. Noti, A. Costantini, E. Garcia-Moruno, Identification of reference genes suitable for normalization of RT-qPCR expression data in Saccharomyces cerevisiae during alcoholic fermentation, Biotechnol. Lett. 33 (2011) 1593–1599, https://doi.org/10.1007/s10529-011-0603-y.

[30] K.J. Livak, T.D. Schmittgen, Analysis of relative gene expression data using real-time quantitative PCR and the $2-\Delta\Delta CT$ method, Methods 25 (2001) 402–408, https://doi.org/10.1006/meth.2001.1262.

[31] M.W. Pfaffl, A new mathematical model for relative quantification in real-time RT-PCR, Nucleic Acids Res. 29 (2001) 45e–445e, https://doi.org/10.1093/nar/29.9.e45.

[32] M. Bradford, A rapid and sensitive method for the quantitation of microgram quantities of protein utilizing the principle of protein-dye binding, Anal. Biochem. 72 (1976) 248–254, https://doi.org/10.1006/abio.1976.9999.

[33] I.-S. Kim, H.-Y. Moon, H.-S. Yun, I. Jin, Heat shock causes oxidative stress and induces a variety of cell rescue proteins in Saccharomyces cerevisiae KNU5377, J. Microbiol. Seoul Korea 44 (2006) 492–501.

[34] J.A. Baron, K.M. Laws, J.S. Chen, V.C. Culotta, Superoxide triggers an acid burst in Saccharomyces cerevisiae to condition the environment of glucose-starved cells, J. Biol. Chem. 288 (2013) 4557–4566, https://doi.org/10.1074/jbc.M112.409508.

[35] R. Serrano, M.C. Kielland-Brandt, G.R. Fink, Yeast plasma membrane ATPase is essential for growth and has homology with (Na+ + K+), K+- and Ca2+-ATPases, Nature 319 (1986) 689–693, https://doi.org/10.1038/319689a0.

[36] E. Navarro-Tapia, A. Querol, R. Pérez-Torrado, Membrane fluidification by ethanol stress activates unfolded protein response in yeasts, Microb. Biotechnol. 11 (2018) 465–475, https://doi.org/10.1111/1751-7915.13032.

[37] T. Grousl, M. Opekarová, V. Stradalova, J. Hasek, J. Malinsky, Evolutionarily conserved 5'-3' exoribonuclease Xrn1 accumulates at plasma membrane-associated eisosomes in post-diauxic yeast, PLoS One 10 (2015) e0122770, https://doi.org/10.1371/journal.pone.0122770.

[38] S. Kubota, I. Takeo, K. Kume, M. Kanai, A. Shitamukai, M. Mizunuma, T. Miyakawa, H. Shimoi, H. Iefuji, D. Hirata, Effect of ethanol on cell growth of budding yeast: genes that are important for cell growth in the presence of ethanol, Biosci. Biotechnol. Biochem. 68 (2004) 968–972, https://doi.org/10.1271/bbb.68.968.

[39] K. Yoshikawa, T. Tanaka, C. Furusawa, K. Nagahisa, T. Hirasawa, H. Shimizu, Comprehensive phenotypic analysis for identification of genes affecting growth under ethanol stress in Saccharomyces cerevisiae, FEMS Yeast Res. 9 (2009) 32–44, https://doi.org/10.1111/j.1567-1364.2008.00456.x.

[40] M. Morard, L.G. Macías, A.C. Adam, M. Lairón-Peris, R. Pérez-Torrado, C. Toft, E. Barrio, Aneuploidy and ethanol tolerance in Saccharomyces cerevisiae, Front. Genet. 10 (2019), https://doi.org/10.3389/fgene.2019.00082.

[41] F. Spira, N.S. Mueller, G. Beck, P. von Olshausen, J. Beig, R. Wedlich-Söldner, Patchwork organization of the yeast plasma membrane into numerous coexisting domains, Nat. Cell Biol. 14 (2012) 640–648, https://doi.org/10.1038/ncb2487.

[42] N.H. Thayer, C.K. Leverich, M.P. Fitzgibbon, Z.W. Nelson, K.A. Henderson, P.R. Gafken, J.J. Hsu, D.E. Gottschling, Identification of long-lived proteins retained in cells undergoing repeated asymmetric divisions, Proc. Natl. Acad. Sci. U.S.A. 111 (2014) 14019–14026, https://doi.org/10.1073/pnas.1416079111.

[43] M. Bagnat, A. Chang, K. Simons, Plasma membrane proton ATPase Pma1p requires raft association for surface delivery in yeast, Mol. Biol. Cell 12 (2001) 4129–4138, https://doi.org/10.1091/mbc.12.12.4129.

[44] G.A. Martínez-Muñoz, P. Kane, Vacuolar and plasma membrane proton pumps collaborate to achieve cytosolic pH homeostasis in yeast, J. Biol. Chem. 283 (2008) 20309–20319, https://doi.org/10.1074/jbc.M710470200.

[45] K.E. Moreira, T.C. Walther, P.S. Aguilar, P. Walter, Pil1 controls eisosome biogenesis, Mol. Biol. Cell 20 (2009) 809–818, https://doi.org/10.1091/mbc.e08-03-0313.

[46] C. Gournas, S. Gkionis, M. M, L. Twyffels, D. Tyteca, B. André, Conformation-dependent partitioning of yeast nutrient transporters into starvation-protective membrane domains, Proc. Natl. Acad. Sci. U.S.A. 115 (2018), https://doi.org/10.1073/pnas.1719462115.

[47] T. Amen, D. Kaganovich, Stress granules sense metabolic stress at the plasma membrane and potentiate recovery by storing active Pkc1, Sci. Signal. 13 (2020), https://doi.org/10.1126/scisignal.aaz6339.

[48] J.R. Buchan, D. Muhlrad, R. Parker, P bodies promote stress granule assembly in Saccharomyces cerevisiae, J. Cell Biol. 183 (2008) 441–455, https://doi.org/10.1083/jcb.200807043.

[49] K.D. Swisher, R. Parker, Localization to, and effects of Pbp1, Pbp4, Lsm12, Dhh1, and Pab1 on stress granules in Saccharomyces cerevisiae, PLoS One 5 (2010) e10006, https://doi.org/10.1371/journal.pone.0010006.

[50] K. Vaškovičová, T. Awadová, P. Veselá, M. Balážová, M. Opekarová, J. Malinsky, mRNA decay is regulated via sequestration of the conserved 5'-3' exoribonuclease Xrn1 at eisosome in yeast, Eur. J. Cell Biol. 96 (2017) 591–599, https://doi.org/10.1016/j.ejcb.2017.05.001.

[51] A. Marcelo, R. Koppenol, L.P. de Almeida, C.A. Matos, C. Nóbrega, Stress granules, RNA-binding proteins and polyglutamine diseases: too much aggregation? Cell Death Dis. 12 (2021) 592, https://doi.org/10.1038/s41419-021-03873-8.